ASEAN Engineering Journal

Full Paper

# LOAD VARIATIONS BASED OPTIMAL REACTIVE POWER SUPPORT FOR HIGH ECONOMIC GAIN IN DISTRIBUTION ELECTRIC POWER NETWORK

R. Senthil Kumar[a], G. Srinivasan[b]*, Rajan. V.R.[c], Lavanya M.[d]

[a]Department of Electrical and Electronics Engineering, SRM Institute of Science and Technology, SRM University, Kattankulathur - 603203, Tamil Nadu, INDIA
[b]Department of Electrical & Electronics Engineering, EXCEL Engineering College, Pallakkapalayam, Komarapalayam – 637303, Namakkal (Dt.), Tamilnadu, INDIA.
[C]Department of Electronics and Communication Engineering, T. John Institute of Technology, Gottigere, Bannerghatta Road, Bangalore - 560083, INDIA.
[d]Department of Mechatronics Engineering, Sona College of Technology, Salem - 636005, Tamil Nadu, INDIA.

**Article history**
Received
27 April 2024
Received in revised form
16 October 2024
Accepted
14 July 2025
Published online
31 August 2025

*Corresponding author
srinivasan_eee@mvjce.edu.in

**Graphical abstract**

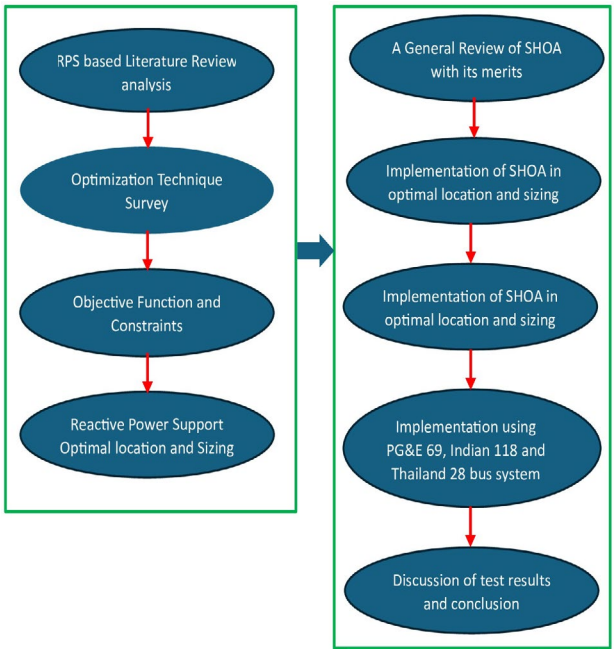


## Abstract

Problems such as high impedance, below normal bus voltages, and Load density of the Distribution Electric Power Network (DEPN) lead to a rise in power losses (real and reactive power losses) with large deviations in node voltage profile. For DEPN planning and operation studies, the power and voltage deviation have been significantly apprehensive. For the past five decades, several researchers have been focusing on DEPN to reduce Power losses to the minimum level. Sitting and sizing of Shunt Capacitor Banks (SSSCB) optimally in the DEPN is of greatest importance in reducing the power losses, power factor improvement, and voltage profile upgradation thereby more Economic Gain (EG). The target of this study is to enhance the performance of the DEPN using Reactive Power Support (RPS) under three different load levels to minimize the capacitor investment cost and maximize the difference in kWh and kVARh using the Sea-Horse Optimizer Algorithm (SHOA). The proposed algorithm has been witnessed with the help of two general test systems (PG&E 69 bus and Indian 118 bus) and one real DEPN (28 bus system, PEA, Thailand). The overall % power loss reduction ranging between 29% and 37% has been observed across the three load variations for all the three test systems. Simulation results reveal that significant improvements in technical and EG are fulfilled which confirms the prospective of the proposed RPS procedure.

*Keywords*: Economic Gain, Distribution Electric Power Network, Power losses reduction, Sea-Horse Optimizer Algorithm, Sitting and Sizing of Shunt Capacitor Banks, Reactive Power Support



## 1.0 INTRODUCTION

The Distribution of Electric Power Network (DEPN) normally suffers from huge power losses, and drops in bus voltages due to insufficient Reactive Power Support (RPS) with a low power factor. Due to the above, the capacity of the main Transformer increases and subsequently increases the investment. Conversely, under overloaded conditions, the power losses are still higher and the bus voltage reaches still worsen. The aforesaid problems can be well mitigated with the help of adequate RPS along the radial DEPN.

To enhance the performance of the DEPN, techniques such as network reconfiguration, real and reactive power compensation, phase balancing series compensation techniques, etc., have been adopted by researchers for the past five decades. However, considering economic aspects and easy implementation methodology, allocation and sizing of shunt capacitors along the DEPN is a viable option to address the above-mentioned problem [1]. From [2], it is understood that economic gain (EG) through

power loss reduction by about 30% with minimum investment cost and minimum grid interventions is possible. Therefore, optimization of reactive power using shunt capacitors in DEPN has been extensively considered in the electrical engineering literature; various published articles are discussed here.

In [3], WGA and PSO have been utilized for the optimal placement and sizing of capacitors in DEPN to minimize both active and reactive power losses. Additionally, [4] introduces an approach for the optimal allocation and determination of capacitor capacities in radial DEPN by employing an exact MINLP model using Mixed-Integer Second-Order Cone Programming (MI-SOCP). This method aims to minimize real power loss in the network.

In [5], the recommendation for achieving optimal allocation and sizing of capacitors in DEPN involves employing the Discrete Vortex Search Algorithm (DVSA) at three specified optimal locations. Meanwhile, [6] proposes the utilization of Chu and Beasley's genetic algorithm (CBGA) along with the General Algebraic Modelling System (GAMS) as an optimization tool for determining the optimal allocation and sizing of capacitors in DEPN. The objective is to minimize both operational and investment costs within the power network. The purpose of [7] is to solve the capacitor investment cost along with energy loss cost together in DEPN using the Slime Mould Optimization Algorithm (SMOA), Bonobo Optimization Algorithm (BOA), and Tunicate Swarm Algorithm (TSA) considering with and without voltage constraint. The authors try to prove that SMOA is better than BOA and TSA in achieving better performance. Ref. [8] discusses the integration of the Quasi-Opposition-Based Learning (QOBL) and Chaotic Local Search (CLS) with the original SFS algorithm that has been developed and applied in radial DEPN to determine the optimal number of buses with appropriate sizing considering both fixed and switched capacitors at different loading conditions. This paper considers two objective functions. The first one deals with energy loss minimization and capacitor cost minimization considering 24 hours and 365 days. In the second objective function, fourteen-hour-based load levels are adopted to evaluate the objective function. PG&E 69 bus, Indian 118 bus, and a Real 152 bus test system have been taken for assessment of the proposed method. In [9], the paper suggests sensitivity indexes and QOSCA to optimize capacitor placement and sizing in DEPN. By employing two equally weighted sensitivity indexes, it identifies key nodes for capacitor placement, and then QOSCA optimizes the capacity of the capacitors to minimize cost, line current, and power losses as a single objective. Optimal allocation and sizing of capacitors in DEPN to solve economic-based objective functions using a multi-objective optimization method has been suggested in [10]. In this work to find optimal nodes for reactive power compensation, two sensitivity-based index such as VSI and PLI have been utilized. Reactive power compensation using the Artificial Electric Field Algorithm (AEFA) in DEPN to reduce energy loss and capacitor purchase cost has been done in [11]. This paper adopted two scenarios.

In the first scenario, the paper employs a Loss Sensitivity Factor (LSF) for optimal node selection, while AEFA (Adaptive Enhanced Firefly Algorithm) has been used to find the optimal sizing of capacitors. The second scenario involves both optimal node selection and sizing carried out by AEFA. The effectiveness of these methods has been demonstrated using the PG&E 69-bus and Indian 118-bus test systems. Additionally, in [12], the paper introduces a strategy utilizing Permutated Oppositional-based Hybrid Differential Evolution (DE) and Sine Cosine Algorithm (SCA) as optimization techniques for the optimal allocation and sizing of capacitors in radial DEPN. The objective is to minimize energy loss cost and capacitor purchase cost across three distinct load variations. The assessment involves the PG&E 69, 85 bus systems, and the Indian 118 bus test system. Moreover, [12] proposes four Sensitivity-Based Indices (SBIs) including the Voltage Stability Index (VSI), power loss index, voltage sensitivity index, and voltage stability margin as part of the Sensitivity-Based Decision-Making Technique (SBDMT) to address the capacitor optimization problem.

Most of the published research articles so far employed sensitivity indexes such as LSF, VSI, and NLSF to locate and sort the most sensitive buses for reactive power compensation. On the other hand, some of the inconveniences faced during the capacitor integration are an independent selection of buses for reactive power optimization and appropriate capacitor sizing could lead to being trapped in local minima instead of global ones [13-15]. Some of the Artificial Intelligence/swarm-intelligence-based bio-inspired optimization techniques have some weaknesses such as partial optimism, scattering problems, suffering from local optimality, requiring large time for simulation, premature or slow convergence in the refined search stage, etc. [16-19]. Hence, there is an obligation to employ a new, uncomplicated, successful, speedy, and proficient Swarm-based Intelligent Meta-heuristic Optimization Technique (SIMOT) to conquer the above demerits.

Ref. [20] proposes the optimal load-shedding problem using hybrid FA and PSO named FAPSO method which has been cand compares its' results with each of FA, PSO, EP and GSA algorithms. Maximization of remaining loads after load shedding process and Voltage Stability Index (VSI) are the objective of this paper. IEEE 33 bus and PSCAD software on part of the Malaysian distribution network with different types of DGs are taken to validate the objective of this paper. Ref. [21] investigates a simultaneous optimization of PVDG output with feeder reconfiguration using EP, PSO, FA and GSA methods considering three different cases. Minimization of net real power loss and voltage profile index and maximization of DG output are the objective of this work. IEEE 33 bus test systems has been taken for evaluation of the proposed optimization methods. Ref. [22] suggests a two-stage fuzzy energy management approach considering optimization and management of multi-parameters of the polygeneration components based on energy, economic, and environmental criteria. . This study also focuses on power loss reduction, reliability improvement, improvement in the sources performance and increase in the energy and cost savings of the system. Off-grid polygeneration system with electric power supply and the on-grid polygeneration with hydrogen vehicle supply are considered in this work.

Proposed Work: This paper engages an application of a new, best, and most durable SIMOT named Sea-Horse Optimizer Algorithm (SHOA) introduced by Shijie Zhao et al. [23] influenced by three activities of sea horses such as natural movement, predation, and breeding has been utilized to solve the technical and economic-based objective function comprising energy losses reduction (kWh and kVArh) with capacitor investment cost under three different load variations. SHOA is a powerful tool for solving a wide range of optimization problems by overcoming challenges faced by other meta-heuristic techniques. Its primary advantage lies in its ability to balance exploration and exploitation effectively, mimicking sea horse behaviors for wide

solution exploration while adapting search patterns for faster convergence. SHOA also uses dynamic interactions and memory to fine-tune solutions, making it highly efficient for complex, high-dimensional problems where other algorithms may struggle with local optima and slow convergence. The principal objective of this work is to achieve maximum EG by proficient optimization of reactive power injections at optimal buses. Capacitor investment cost related to heavy load level has only been considered in this paper for EG calculation purposes. To substantiate the effectiveness of the suggested algorithm, three test systems such as real 28 bus DEPN (PEA, Thailand), PG&E 69 bus test system, and Indian 118 bus test system have been taken considering load variations.

Purpose and Contribution: With the above-discussed features, the contributions of this work include *(i) Suggesting the best and most robust SIMOT called SHOA to solve the economical-based objective function considering three different load levels. (ii) Cost-based assessment of real and reactive power loss reduction with capacitor purchase cost and (iii) For the first time, optimal placement and sizing of capacitors considering 28-bus PEA, Thailand DEPN.*

The remainder of this work has been ordered as follows: Section 2 presents the problem construction in terms of objective functions and load flow. Section 3 demonstrates the developed optimization method with its ability to solve the economic-based objective. Section 4 discusses the numerical results obtained by the presented method and the concluding remarks are reported in Section 5.

## 2.0 FORMULATION OF OBJECTIVE FUNCTION

This research aims to maximize the EG by SSSCB optimally in three radial DEPNs while meeting both system equality and inequality constraints. Before discussing the objective function, let's discuss the DEPN Power Flow (DEPNPF) used in this work.

### 2.1 Distribution Electric Power Network Power Flow (DEPNPF)

To appraise the efficiency of the DEPN under normal operating conditions, a Power Flow (PF) has been performed frequently to identify the requirement of additional power supply necessary to satisfy during seasonal periods, the necessity of reactive power support, and to ensure the bus voltage profiles within the acceptable limits. Matrix-based load flow methods like Gauss-Seidel, Newton-Raphson, and Fast-Decoupled have proven ineffective in solving DEPN due to the high R/X ratio and radial topology [24,25]. This paper utilizes the efficient, robust, adaptable, and versatile DEPNPF method, developed in 2003 [26], which is based on recursive functions and a linked-list data structure to effectively address the problem of reactive power optimization. Total real and reactive power loss (by summing up all the branches of the radial DEPN, which includes laterals and sub-laterals) of the entire DEPN may be expressed as given below:

$$P^{LT} = \sum_{a=1}^{tnb} P_{Loss(a)} \quad (1)$$

$$Q^{LT} = \sum_{a=1}^{tnb} Q_{Loss(a)} \quad (2)$$

Where $P_{Loss(a)} = \frac{P_{(a+1)}^2 + Q_{(a+1)}^2}{\left|V_{(a)}^2\right|} \times R_{(a,\,a+1)}$ and

$$Q_{Loss(a)} = \frac{P_{(a+1)}^2 + Q_{(a+1)}^2}{\left|V_{(a)}^2\right|} \times X_{(a,\,a+1)}$$

$P^{LT}$ and $Q^{LT}$ are the sum of real and reactive power losses of all the branches of the DEPN. $P_{a+1}$ and $Q_{a+1}$ represents the real and reactive power flow of the $(a+1)^{th}$ branch in kW, kVAr respectively. $R_a$ and $X_a$ are the resistance and inductance of the branch connecting 'a' and 'a+1' in Ω. 'tnb' indicates the total number of branches in the DEPN.

### 2.2 Problem Statement

The main objective of the proposed work is to increase the difference in power losses reduction obtained before and after optimal reactive power support while satisfying the equality and inequality constraints. The objective function has been indicated in (3) and the necessary constraints have been mentioned from (4) through (7).

Maximize $F = \sum_{lv=1}^{NLV} [F_1 + F_2 + F_3]_{lv}$ (3)

Where $F_1 = \lambda_1 \times \sum_{lv=1}^{NLV} T_l \times \left[\frac{P_{(ICDN)}^{LT} - P_{(ACP)}^{LT}}{P_{(ICDN)}^{LT}}\right]_{lv}$,

$$F_2 = \lambda_2 \times \sum_{lv=1}^{NLV} T_l \times \left[\frac{Q_{(ICDN)}^{LT} - Q_{(ACP)}^{LT}}{Q_{(ICDN)}^{LT}}\right]_{lv}$$

$$F_3 = \lambda_3 \times \left[\frac{\left(Q_{TD}^{(lv)} + Q_{ICDN}^{LT(lv)}\right) \times C_{QL}}{\left(\sum_{s=1}^{NQN} Q_{C(s,lv)} \times C_{cap}\right) + \left((C_{O\&M} + C_{ins}) \times NQN\right)}\right]$$

subject to equality constraints

$$Q_{(ACP)}^{ES(lv)} - Q_{TD}^{(lv)} + \sum_{s=1}^{NQN} Q_{C(s,lv)} - Q_{(ACP)}^{LT(lv)} = 0 \quad (4)$$

Inequality Constraints

$$\sum_{s=1}^{NQN} Q_{C(s,lv)} \le (Q_{TD}^{(lv)} + Q_{(ACP)}^{LT(lv)}) \quad (5)$$

$$Q_{C(lv)}^{\min} \le Q_{C(lv)} \le Q_{C(lv)}^{\max} \quad (6)$$

$$V_k^{\min} \le V_k \le V_k^{\max} \quad (7)$$

## 3.0 PROPOSED OPTIMIZATION METHOD (SHOA) [23]

### 3.1 Sea Horse Optimizer Algorithm (SHOA)- An Overview

The Sea Horse Optimization Algorithm (SHOA) draws its inspiration from the behavior of seahorses as they navigate the ocean in search of prey and engage in movement and breeding activities. The SHOA incorporates the fundamental principles of exploration and exploitation often seen in meta-heuristic methods. It achieves this by emulating the social behavior observed in seahorses, particularly in terms of their movement

and their search for prey in the underwater environment.

The SHOA comprises three essential elements: movement, predation, and breeding. These components are designed to balance exploring new solutions and exploiting the current ones. To elaborate, the algorithm employs local and global search strategies for the movement and predation phases, respectively. Additionally, the breeding behavior occurs once the first two behaviors are completed. Now, let's break down these components further in mathematical terms and discuss their details.

### 3.1.1 Initialization

In the SHOA, similar to other meta-heuristic algorithms, the initial population setup involves viewing each sea horse as a potential solution within the problem's search space. This population of sea horses can be concisely represented mathematically as:

$$S_h = \begin{pmatrix} x_{1,a} & \cdots & x_{1,d} \\ \vdots & \ddots & \vdots \\ x_{n,a} & \cdots & x_{n,d} \end{pmatrix} \quad (8)$$

$$S_h = rand \times (U_{B,i} - L_{B,i}) + L_{B,i} \quad (9)$$

Where 'd' is the dimension of variables and represents the seahorse with 'n' as the population size. The upper ($U_{B,i}$) and lower ($L_{B,i}$) limits for potential solutions are determined as random results for each individual. A crucial component involves introducing random values from 0 to 1, denoted as rand. Within the population, there are individuals known as $Sh_{elite}$, which possess a minimum level of fitness and represent top candidates.

### 3.1.2 Movement Behavior of Sea horses

Sea horses exhibit various movement patterns during their natural behaviors, and these patterns are often described by a normally distributed random distribution with a mean of 0 and a standard deviation of 1. To strike a balance between exploration and exploitation in the optimization process, a cut-off point is introduced. This cut-off point divides the distribution into two halves: one for local exploration and the other for global search. Consequently, the subsequent phases of the algorithm are designed to characterize and utilize these movement behaviors effectively.

Stage 1: In the SHOA, the spiral movement of sea horses is akin to the vortex in the ocean. When a normal random value falls on the right side of the cut-off point, it's primarily used for local exploration. In this phase, sea horses follow a spiral motion toward the best solution $X_{best}$. Importantly, this movement employs a Lévy flight to model the step size, a strategy beneficial for sea horses as it enhances their chances of venturing into different areas, especially in the early stages of the optimization process. This approach also prevents the SHOA from overly focusing on a single location. Furthermore, the sea horse's spiral motion continuously adjusts its rotation angle to expand the search around the current local solutions, thus increasing the chances of finding optimal solutions.

$$x_{new}^{t+1} = x_a^t + Levy(\lambda)((x_{best}^t - x_a^t) \times x \times y \times z) + x_{best}^t \quad (10)$$

Subject to the constraints

$$x = p \times \cos\alpha \quad (11)$$

$$y = p \times \sin\alpha \quad (12)$$

$$z = p \times \alpha \quad (13)$$

$$p = u \times e^{\alpha v} \quad (14)$$

$$\alpha = rand \times 2\pi \quad (15)$$

In the spiral movement context, the variables x, y, and z denote the three-dimensional coordinates corresponding to the positions of the search agents. These coordinates are vital in updating the agents' positions as they progress through the optimization process. The length of the spiral stems (p) has been determined by the logarithmic spiral constants 'u' and 'v', both set to 0.05. These constants regulate the shape and size of the spiral movement followed by the agents during their exploration. Additionally, the value of α is randomly chosen from the range [0, 2π]. To model the Lévy flight distribution function, denoted as $L_Z$, the following equation is employed:

$$L_Z = S \times \left( \frac{\omega \times \sigma}{|K|^{\frac{1}{\lambda}}} \right) \quad (16)$$

This equation governs the step size of the sea horse's movement in the algorithm, influencing the agents' exploration of the search space. $\omega$ and K are random variables in the range 0 to 1. The value of λ is randomly chosen between 0 and 2and constant S is set at 0.01.

$$\sigma = \left( \frac{\Gamma(1+\lambda) \times \sin\left(\frac{\pi\lambda}{2}\right)}{\Gamma\left(\frac{1+\lambda}{2}\right) \times \lambda \times 2^{\left(\frac{\lambda-1}{2}\right)}} \right) \quad (17)$$

Stage 2: The sea horse's Brownian motion in response to ocean waves is simulated in this algorithmic stage. The SHOA performs a drifting search operation when the random value falls to the left of the cut-off point. The search procedure becomes essential in this situation to avoid the SHOA becoming trapped at the local extrema. Brownian motion is used, expanding the sea horse's movement to enable a more effective investigation of the search space. The equation given below describes the mathematical formulation for this feature as follows:

$$x_{new}^{t+1} = x_a^t + rand \times l \times \beta_t \times (x_a^t - \beta_a \times x_{best}^t) \quad (18)$$

Where $\beta_t = \frac{1}{\sqrt{2\pi}} e^{\left(-\frac{x^2}{2}\right)}$

In this context, "*l*" represents a constant coefficient set to 0.05, and the Brownian motion random walk coefficient is denoted by

$$x_{new}^{t+1} = \begin{cases} x_a^t + levy(\lambda)((x_{best}^t - x_a^t) \times x \times y \times z) + x_{best}^t, r_1 > 0 \\ x_a^t + rand \times l \times \beta_t \times (x_a^t - \beta_a \times x_{best}^t), r_1 \le 0 \end{cases} \quad (19)$$

### 3.1.3 Predation Behavior of Sea Horses

In the SHOA, the success or failure of capturing prey, represented by zooplankton or tiny crustaceans, has been determined by a random number compared against a threshold value of 0.1. Successful predation signifies the SHOA's adeptness in exploiting the environment, offering insights into the general location of its prey, often referred to as "the best" within the search space.

When $r_2$ surpasses 0.1, it indicates the sea horse's successful predation. In this case, it skillfully approaches its target (the best solution), overtakes it, and ultimately captures it. However, if predation fails and $r_2$ is less than or equal to 0.1, both the sea horse and the target exhibit a reverse response, implying that the sea horse is likely to continue exploring the vicinity in search of prey. This predation behavior is mathematically represented by the Equation below

$$x_{new,2}^{t+1} = \begin{cases} \delta \times (x_{best} - rand \times x_{new}^{t}) + (1-\delta) \times x_{best}, r_2 \geq 0.1 \\ (1-\delta) \times (x_{new}^{t} - rand \times x_{best}) + \delta \times x_{new}^{t}, r_2 \leq 0.1 \end{cases} \quad (20)$$

Where $$\delta = \left(1 - \frac{t}{T_{\max}}\right)^{\frac{2t}{T_{\max}}}$$

Here, $r_2$ represents a randomly generated integer value within the range [0, 1], and $x_{new}^{t}$ denotes the sea horse updated position after t[th] iteration. To adjust the sea horse's step size for prey pursuit, it progressively decreases over iterations. This step size reduction is determined using the Equation below, where $T_{\max}$ represents the maximum number of iterations in the optimization process. This approach allows the sea horse to fine-tune its movements as the optimization process progresses.

### 3.1.4 Breeding Behavior of Sea Horses

In the SHOA, the population is divided into male and female groups based on their fitness levels. Among these sea horses, the males take on the breeding responsibility. The algorithm selects the top half of the population with the highest fitness scores as fathers, while the remaining half serves as mothers in the reproductive process. This approach ensures that individuals with better fitness contribute to the genetic diversity and evolution of the population, aligning with principles of natural selection and optimization.

$$F(s) = X_{sort}^{2}\left(1 : \frac{p}{2}\right) \quad (21)$$

$$M(s) = X_{sort}^{2}\left(\frac{p}{2} + 1 : p\right) \quad (22)$$

In the SHOA approach, sea horse positions referred to as $F(s)$, are sorted by fitness values. The population is divided into male (fathers) and female (mothers) groups. Random mating between these groups produces one offspring per pair for efficiency in the algorithm's execution, ensuring genetic diversity and optimization.

$$x_a^{new\_born} = r_3 \times x_a^{F} + (1 - r_3) \times x_a^{M} \quad (23)$$

Where $r_3$ is randomly chosen from the range 0 to 1. Male and female members are randomly selected and represented as $x_a^F$ and $x_a^M$ respectively.

## 3.2 Implementation of SHOA for RPI

The proposed SHOA has been applied to determine the optimal allocation and capacity of capacitors in three EDPNs. The objective is to minimize both real power loss and reactive power loss while enhancing bus voltage. The SHOA involves the following steps:

**Step 1:** Initialize the boundary limits for variables, which include the optimal capacitor allocation location and size, and specify the maximum number of iterations ($N_{\max}$) and population ($p$). Generate initial solution vectors that take into account all constraints (4) - (7).

**Step 2:** Compute network parameters, including real power loss, reactive power loss, and voltages at all nodes, for each solution vector (SV) generated using the EDPNPF method described in ref. [23].

**Step 3:** Compute the fitness of each sea horse and find the best sea horse $X_{best}$.

**Step 4:** When $r_1$ is at the right side of the vortex (local search), Generate the levy coefficient and update the position of sea horses using equations using (10) and (16) respectively.

**Step 5:** When $r_1$ is at the left side of the vortex (global search), update each sea horse position using (18).

**Step 6:** Equation (20) is used to update the sea horse's position during the predation phase and the fitness of each sea horse has been evaluated.

**Step 7:** Using (21) and (22), select the parent population. Generate offspring using (23) and select offspring ranking top with the highest fitness as the next set of population.

**Step 8:** The iteration process stops after the successful completion of the final iteration. The final value of the objective function (EG in $) with the capacitor variable values will be displayed. Otherwise, steps 2 to 7 will be repeated till the maximum value of the objective function is obtained. Art. 3.3 displays the pseudo-code and Art. 3.4 shows the flow chart for the proposed reactive power optimization problem using SHOA. In the SHOA, the population is divided into male and female groups based on their fitness.

## 3.3 Pseudo Code for RPI problem - SHOA

The pseudocode for the algorithm implementation is given below.

1. Initialize Sea horses $X_i = (1, 2, ..N)$, $p$ and $N_{\max}$
2. Calculate the fitness of each horse and find the best
3. while (t < $N_{\max}$) do
4. /*movement behaviour*/
5. If = randn > 0 do
6. Set u= v= 0.05 and randn ϵ ( 0, 2Π)

```
7. Generate Levy coefficient using eqn.16
8. update sea horse position using eqn. 10
9. else if do
10. update sea horse position using eqn.18
11. end if
12. /* predation behaviour*/
13. Update Sea horse position using eqn. 20
14. Calculate the fitness value of each sea horse
15. /* breeding behaviour*/
16. Select parents using eqn.21 and 22
17. Generate offspring using eqn.23
18.  Calculate the fitness of the new offspring
19. Select the next generation population using the offspring and parents
from the top of the rank list
20. Update
21. i=i+1
22. end while
```

### 3.4 Flow chart

The flowchart depicting the SHOA-based capacitor allocation for optimal reactive power support is shown below.

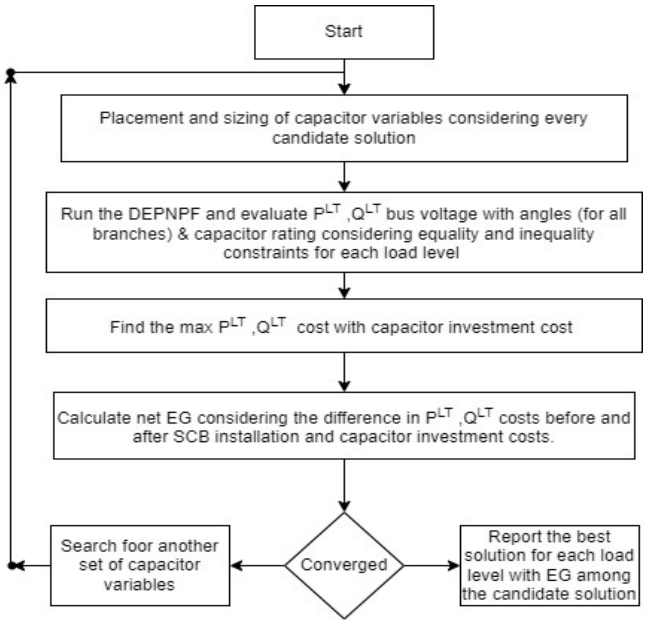


## 4.0 CASE STUDY DETAILS, SIMULATION RESULTS AND DISCUSSIONS

To validate the SHOA's optimization effectiveness, simulations have been conducted on three radial test DEPNs. Load variations of 0.7 p.u. and 1.0 p.u. are considered for the 28-bus test system of Kalasin feeder 5, PEA, Thailand. Additionally, the PG&E 69-bus system and Indian 118-bus test system were tested with load variations of 0.5 p.u., 1.0 p.u., and 1.6 p.u. for the former and 0.75 p.u., 1.0 p.u., and 1.25 p.u. for the latter test systems. These simulations aimed to showcase the SHOA's optimization capabilities across diverse load conditions in different power network configurations. The details of the three DEPNs and the simulation results have been discussed in Art. 4.1 to 4.3.

Node number 1 has been taken as a substation/slack bus for all the DEPN. All nodes, except bus no. 1, are considered as load nodes. The voltage for bus number 1 has been fixed as 1 p.u. RPS has been expected to be applied from node 2 through the end node of the DEPN. The proposed algorithm using DEPNPF has been developed and executed in MATLAB software, running on an i5 Intel processor with 8 GB RAM. The solution vector size and the number of iterations have been set to 800 and 100, respectively. Two variables are assigned per RPS (optimal node and optimal sizing) considering three load variations and the optimal node number must be the same for all three load variations.

The cost of real power energy cost has been taken as $0.05 / kWh. According to ref. [27], the cost of reactive energy loss (kVArh) is one-third of the cost of reactive power. The capacitor's purchase cost stands at $5 per KVAr, with installation and maintenance expenses set at $620 per node [28]. Across all DEPNs, a base MVA of 100 MVA has been adopted. The base kV is 22 kV for Thailand's 28-bus test system, 12.66 kV for the PG&E 69-bus test system, and 11 kV for the Indian 118-bus test system. To assess the effectiveness of the proposed method in reducing power loss while considering capacitor investment costs, simulations have been conducted across all DEPNs under three distinct load variations. Exploring the impact of EGs on the three DEPNs, SSSCBs were carried out at three optimal locations for the real 28-bus Thailand test system and the PG&E 69-bus test system. For the Indian 118-bus test system, SSSCBs were selected at eight specific locations. In this work, the capacitor sizing has been considered as discrete values in steps of 25 KVAr. Capacitor investment cost related to heavy load variation has only been considered for cost evaluation. The values of λ1, λ2, and λ3 are considered as 0.6, 0.3, and 0.1 respectively.

### 4.1 28-Bus Test System (Kalasin Feeder 5 Of PEA, Thailand) – Results and Discussions

The developed SHOA has been tested on Kalasin feeder 5 of PEA, Thailand which has 28 buses, 27 branches, and 19 load buses. The data for this DEPN can be obtained from [29]. The single-line diagram for the practical 28-bus test system is depicted in Figure 1. The total apparent power demand under two load variations (0.7 p.u. and 1.0 p.u.) are (2800 + j 1735) kVA and (3998.8 + j2478.2) kVA respectively which are taken from [29]. The real and reactive power losses under the Initial Condition of the Distribution Network (ICDN) are (59.03 +j 112.16) and (124.426+j 236.436) kVA respectively [29]. The minimum bus voltage under ICDN is 0.9637 p.u. and 0.9472 p.u. respectively considering two load variations [29]. The total power losses cost under ICDN are $41370.34 and $26203.544 per annum respectively. The duration of the two load variations (0.7 p.u. and 1.0 p. u) are taken as 11 hrs. and 13 hrs. per day [29] respectively.

From Table 1 it is evidenced that RPS under two load variations yields real and reactive power loss reductions between 29.2% and 30.5% respectively with reactive power penetration of around 87%. The difference in minimum bus voltage recorded After Capacitor Placement (ACP) is 0.0166 p.u. and 0.0244 p.u. respectively. From Table 1, it is apparent that the net EG yielded by SHOA considering two load variations is found to be $7607.8. Figure 2 depicts the performance of SHOA in bus voltage enhancement under ICDN and ACP considering two load variations.

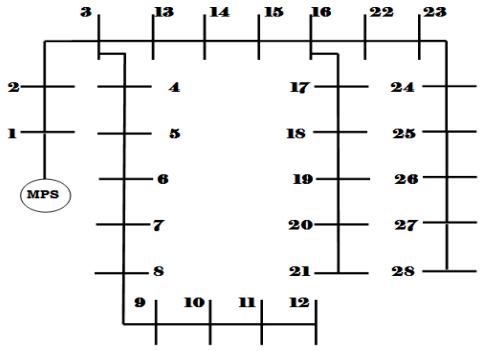


**Figure 1** Kalasin feeder 5 of PEA, Thailand – ICDN

**Table 1** Performance of SHOA considering load variations – 28-node PEA, Thailand DN.

| Load level | 0.7 p.u. | 1.0 p.u. |
|---|---|---|
| $P_{Loss\ (ACP)}$ / $P_{Loss\ (ICDN)}$ (kW) | 41.78 / 59.03 | 86.5851 / 124.426 |
| % $P_{Loss}$ reduction | 29.2217 | 30.4122 |
| $Q_{Loss\ (ACP)}$ / $Q_{Loss\ (ICDN)}$ (kVAr) | 79.29 / 112.16 | 164.324 / 236.436 |
| % $Q_{Loss}$ reduction | 29.3053 | 30.5 |
| Capacitor details (kVAr) | 225 (8)<br>250 (17)<br>1025 (25) | 325 (8)<br>400 (17)<br>1450 (25) |
| % Cap. Penetration | 86.4686 | 87.7657 |
| $V_{min}$ (p.u) | 0.9803 | 0.9716 |
| T × Δ $P_{Loss}$ Cost ($) | 3462.837 | 8977.6824 |
| T × Δ $Q_{Loss}$ Cost ($) | 2199.444 | 5702.834 |
| Cap. Inv. Cost ($) | 12735 | |
| Net E G ($) | **7607.8** | |

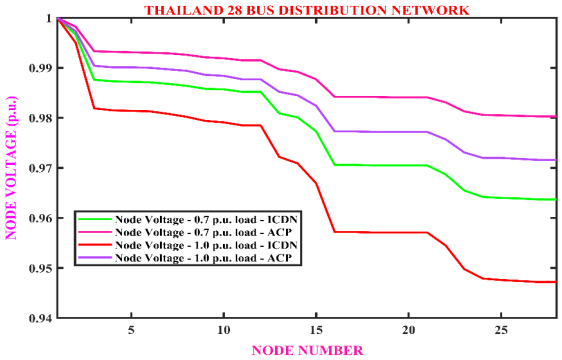


**Figure 2** Bus Voltage profile enhancement – 2 load variations – Real 28-bus PEA, Thailand

## 4.2 PG&E 69-Bus Test System – Results and Discussions

The next test system considered here is the PG&E 69-bus test system which has 69 buses and 68 sectionalizing switches and five tie-switches. The total real and reactive power demand is under 0.5 p.u., 1.0 p.u. and 1.6 p.u. load variations are 2385.2122 kVA, 4903.0477 kVA, and 8157.72 kVA at 0.818494, 0.821365, and 0.825527 power factor lagging. The real and reactive power losses with minimum bus voltage under ICDN considering three load variations are (51.5822 +j 23.54) kVA, (225 + j102.14) kVA and (652.22 +j 294.114) kVA with a minimum bus voltage of 0.9567 p.u., 0.90919 p.u. and 0.8445 p.u. respectively. The duration of the three load levels (LLV, MLV, and HLV) have been considered as 6 hrs., 13 hrs., and 5 hrs. per day respectively. The total real and reactive power loss costs under ICDN are $118544.257 and $17882.7553 per year respectively. Figure 3 shows the single-line diagram of the PG&E 69-bus test system.

Table 2 reveals the performances of the PG&E 69-bus test system under three different load variations mentioned previously. From Table 2 it is clear that the real and reactive power loss reductions are found to be between 32% and 38% with a reactive power penetration between 61% and 68%. The differences in minimum bus voltage recorded are 0.0094 p.u., 0.02201 p.u. and 0.0399 p.u. respectively considering three load variations. By calculating the net EG ACP at three locations, it is observed that a net gain of $33605.393 has been attained considering three load variations. Figure 4 shows the bus voltage enhancements under ICDN and ACP considering three load variations.

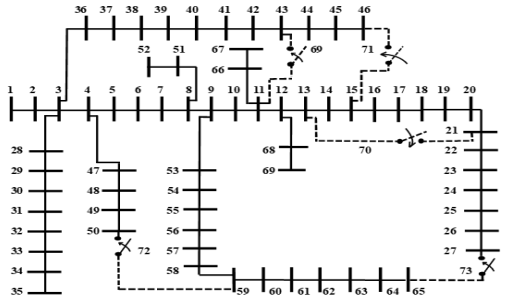

**Figure 3** PG&E 69-bus test system - ICDN.

**Table 2** Performance of SHOA considering load variations – PG&E 69-bus DN.

| Load level | 0.5 p.u. | 1.0 p.u. | 1.6 p.u. |
|---|---|---|---|
| $P_{Loss}$ (ACP) / $P_{Loss}$(ICDN) (kW) | 34.157/ 51.5822 | 145.225 / 225 | 405.4283 / 652.2165 |
| %$P_{Loss}$ reduction | 33.78142 | 35.4555 | 37.8384 |
| $Q_{Loss}$ (ACP) / $Q_{Loss}$(ICDN) (kVAr) | 16.0145 / 23.541 | 67.6024 / 102.1155 | 187.8515 / 294.1142 |
| %$Q_{Loss}$ reduction | 31.972 | 33.7 | 36.123 |
| Capacitor details (kVAr) | 125 (12)<br>125 (21)<br>575 (61) | 425(12)<br>175 (21)<br>1225 (61) | 475 (12)<br>350 (21)<br>2000 (61) |
| %Cap. penetration | 61.256 | 67.7532 | 65.5483 |
| $V_{min}$ (p.u) | 0.9661 | 0.9313 | 0.8844 |
| T × Δ $P_{Loss}$ Cost ($) | 1908.06 | 18926.62 | 22519.423 |
| T × Δ $Q_{Loss}$ Cost ($) | 274.7173 | 2729.411 | 3232.1572 |
| Cap. Inv. Cost ($) | | **15985** | |
| Net E G ($) | | **33605.393** | |

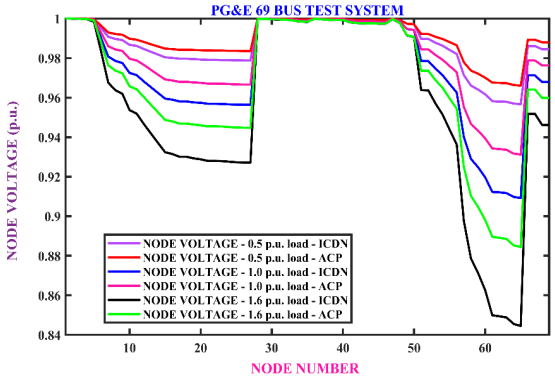


**Figure 4**. Bus Voltage profile enhancement – 3 load variations – PG&E 69-bus system

Tables 3 to 6 expose the comparison of the performance of other optimization techniques with SHOA under LLV, MLV, and HLV. From Table 3, it is witnessed that the performance of SHOA under LLV yields better performance in terms of real and reactive power loss reduction and bus voltage enhancement compared to [3,7]. The real power loss reduction achieved by WoVC [7] is 0.03013% better than the proposed technique. However, it is to be noted the increase in real power loss reduction is found to be minuscule, and also the capacitor penetration is 75 kVAr more than SHOA. The reactive power loss reduction is also found to be better than [3]. The bus voltage improvement is almost equal to other techniques.

Table 4 discloses the performance of SHOA under MLV compared with [3 – 7]. It is visible from Table 4 that the real and reactive power loss reduction achieved by SHOA is better than [3 – 7]. The minimum bus voltage enhanced by SHOA is better than [3 – 7]. However, WGA [3] and WVC [7] achieve a better performance than SHOA in terms of bus voltage enhancement. Table 5 compares the effect of RPS under HLV. The real and reactive power loss attained by the proposed method is better than [3,7]. But it is to be noted that the capacitor penetration achieved by SHOA is more than [3, 7(WoVC)]. The minimum bus voltage enhancement achieved by SHOA is better than [3,7] except for SMOA (WVC) [7].

**Table 3** Comparison of SHOA – PG&E 69-bus DN – LLV (0.5 p.u.).

| Parameters | WGA [3] | PSO [3] | SMOA [7] | | BOA [7] (WVC) | TSA [7] (WVC) | SHOA |
|---|---|---|---|---|---|---|---|
| | | | WoVC | WVC | | | |
| $P_{Loss}$ (ACP) / $P_{Loss}$ (ICDN) (kW) | 34.84 / 51.58 | 36.51 / 51.58 | 34.14 / 51.58 | 34.42 / 51.58 | 34.4144 / 51.58 | 34.6901 / 51.58 | 34.157 / 51.5822 |
| % $P_{Loss}$ reduction | 32.45444 | 29.2167 | 33.81155 | 33.2687 | 33.2796 | 32.74506 | 33.78142 |
| $Q_{Loss}$ (ACP) / $Q_{Loss}$ (ICDN) (kVAr) | 16.33 / 23.54 | 16.76 / 23.54 | --------- | --------- | --------- | --------- | 16.0145 / 23.541 |
| % $Q_{Loss}$ reduction | 30.62872 | 28.80204 | --------- | --------- | --------- | --------- | 31.972 |
| Capacitor details (kVAr) | 598 (63)<br>149 (23)<br>12.2 (27) | 83 (18)<br>86.4 (24)<br>642.5 (57) | 150 (12)<br>150 (18)<br>600 (61) | 200 (16)<br>500 (61)<br>100 (64) | 300 (16)<br>400 (61)<br>200 (64) | 100 (15)<br>400 (61)<br>200 (64) | 125 (12)<br>125 (21)<br>575 (61) |
| % Cap. Penetration | 56.37 | 60.28364 | 66.8251 | 59.4 | 66.8251 | 51.975 | 61.256 |
| T × $\Delta P_{Loss}$ Cost ($) | 1833.03 | 1650.165 | 1909.68 | 1879.02 | 1879.633 | 1849.444 | 1908.06 |
| $V_{min}$ (p.u) | 0.9668 | 0.9519 | 0.967 | 0.97 | --------- | --------- | 0.967 |

**Table 4** Comparison of SHOA – PG&E 69-bus DN – MLV (1.0 p.u.).

| Parameters | WGA [3] | PSO [3] | MI-SOCP/ DVSA [4,5] | CBGA [6] | SMOA [7] | | BOA [7] (WVC) | TSA [7] (WVC) | SHOA |
|---|---|---|---|---|---|---|---|---|---|
| | | | | | WoVC | WVC | | | |
| $P_{Loss}$ (ACP) / $P_{Loss}$ (ICDN) (kW) | 148.70 / 224.96 | 165.23 / 224.96 | 145.397/ 225.072 | 145.37 / 225 | 145.78 / 225 | 146.2 / 225 | 146.691 / 225 | 146.5182 / 225 | 145.225 / 225 |
| % $P_{Loss}$ reduction | 33.9 | 26.55139 | 35.3998 | 35.39 | 35.2089 | 35.02222 | 34.804 | 34.8808 | 35.4555 |
| $Q_{Loss}$ (ACP) / $Q_{Loss}$ (ICDN) (kVAr) | 69.38 / 101.99 | 75.38 / 101.99 | -------- | ------- | -------- | --------- | -------- | -------- | 67.6024 / 102.1155 |
| % $Q_{Loss}$ reduction | 31.9737 | 26.091 | -------- | ------- | -------- | --------- | -------- | -------- | 33.7 |
| Capacitor details (kVAr) | 1197 (63)<br>300 (23)<br>22.5(27) | 288.8 (18)<br>122 (24)<br>900 (57) | 300 (11)<br>300 (18)<br>1200 (61) | 450 (12)<br>150 (22)<br>1200(61) | 150 (12)<br>300 (18)<br>1800(61) | 400 (16)<br>1100(61)<br>200 (64) | 600 (12)<br>1200(61)<br>400 (64) | 400 (15)<br>900 (61)<br>0 (64) | 425(12)<br>175 (21)<br>1225(61) |
| % Cap. Penetration | 56.4115 | 48.6635 | 66.8251 | 66.8251 | 83.5313 | 63.1126 | 81.6751 | 48.2625 | 67.7532 |
| T × $\Delta P_{Loss}$ Cost ($) | 18092.685 | 14170.943 | 18902.9 | 18892.22 | 18794.945 | 18695.3 | 18578.8 | 18619.8 | 18926.62 |
| $V_{min}$ (p.u) | 0.9315 | 0.93 | 0.93 | --------- | 0.93 | 0.932 | --------- | --------- | 0.9313 |

**Table 5** Comparison of SHOA – PG&E 69-bus DN – HLV (1.6 p.u.)

| Parameters | WGA [3] | PSO [3] | SMOA [7] | | BOA [7] (WVC) | TSA [7] (WVC) | SHOA |
|---|---|---|---|---|---|---|---|
| | | | WoVC | WVC | | | |
| $P_{Loss}$ (ACP) / $P_{Loss}$ (ICDN) (kW) | 417.83 / 648.9 | 446.48 / 648.9 | 413.93 / 652.2 | 441.66 / 652.2 | 442.4536 / 652.2 | 441.6815 / 652.2 | 405.4283 / 652.2165 |
| % $P_{Loss}$ reduction | 35.6095 | 31.19433 | 36.5333 | 32.28151 | 32.15983 | 32.2782 | 37.8384 |
| $Q_{Loss}$ (ACP) / $Q_{Loss}$ (ICDN) (kVAr) | 193.74 / 292.71 | 201.34 / 292.71 | -------- | --------- | --------- | --------- | 187.8515 / 294.1142 |
| % $Q_{Loss}$ reduction | 33.8116 | 31.2152 | -------- | --------- | --------- | --------- | 36.123 |
| Capacitor details (kVAr) | 1797 (63)<br>449 (23)<br>34.2 (27) | 547.1 (18)<br>175.5 (24)<br>900 (57) | 150 (12)<br>300 (18)<br>1800 (61) | 700 (16)<br>1400 (61)<br>1400 (64) | 700 (15)<br>1400 (61)<br>1400 (64) | 700 (12)<br>1400 (61)<br>1400 (64) | 475 (12)<br>350 (21)<br>2000 (61) |
| % Cap. Penetration | 52.90733 | 37.649 | 52.2066 | 81.2103 | 81.2103 | 81.2103 | 65.5483 |
| T × $\Delta P_{Loss}$ Cost ($) | 21085.14 | 18470.825 | 21742.14 | 19211.775 | 19139.36 | 19209.813 | 22519.423 |
| $V_{min}$ (p.u) | 0.8833 | 0.8726 | 0.88 | 0.9 | -------- | -------- | 0.8844 |

**Table 6** Comparison of SHOA – PG&E 69-bus DN – All load variations combined

| Parameters | WGA [3] | PSO [3] | SMOA [7] | | BOA [7] (WVC) | TSA [7] (WVC) | SHOA |
|---|---|---|---|---|---|---|---|
| | | | WoVC | WVC | | | |
| Total $\Delta P_{Loss}$ cost / Year ($) | 41010.715 | 34291.933 | 42446.765 | 39786.095 | 39597.803 | 39679.067 | 43354.103 |
| Total $\Delta Q_{Loss}$ cost / Year ($) | 5852.411 | 5131.05 | -------- | --------- | --------- | --------- | 6236.29 |
| Cap. Inv. Cost ($) | 13261 | 9973 | 13110 | 19360 | 19360 | 19360 | 15985 |
| Net E G ($) – considering only $\Delta P_{Loss}$ cost ($) | -------- | --------- | **29336.765** | **20426.095** | **20237.803** | **20319.067** | **27369.103** |
| Net EG ($) – considering $\Delta P_{Loss}$ cost and $\Delta Q_{Loss}$ cost | **33602.126** | **29449.983** | -------- | --------- | --------- | --------- | **33605.393** |

However, WGA [3] and WVC [7] achieve a better performance than SHOA in terms of bus voltage enhancement. Table 5 compares the effect of RPS under HLV. The real and reactive power loss attained by the proposed method is better than [3,7]. But it is to be noted that the capacitor penetration achieved by SHOA is more than [3, 7(WoVC)]. The minimum bus voltage enhancement achieved by SHOA is better than [3,7] except for SMOA (WVC) [7].

The solutions obtained by the proposed method under three load variations (combined) have been compared with [3,7]. It is found from Table 6 that the achieved solutions by SHOA confirm the superiority of the presented method in determining the efficient RPS by achieving better EG. However, SMOA (WoVC) [7] yields a better solution than the SHOA because of the decrease in capacitor values optimized by [7].

### 4.3 Indian 118-Bus Test System – Results and discussions

Finally, the proposed method has been applied on a large-scale Indian 118 bus EDPN. It has 118 nodes, 117 branches, 3 laterals, and 11 sub-laterals. The KV (base) and MVA (base) for this test system are 11 KV and 100 MVA respectively. The total apparent power demand for this test system under three load variations are (17.0323 + j 12.7733), (22.70972 +j 17.0411) and (28.38715 +j 21.288835) MVA respectively. The apparent power loss under three load variations is (697.91615 +j 527.4), (1300 + j 979.0453), and (2136.71335 + j 1604.6151) KVA respectively. The minimum bus voltages under ICDN are 0.90489, 0.8688 and 0.829565 p.u. @ bus no. 77 respectively. The net total real and reactive power losses cost per year under ICDN are $579821.9116 and $145483.3084 respectively. Similar to the previous test system, the hours pertaining to LLV, MLV, and HLV per day have been considered as 6 hrs., 13 hrs., and 5 hrs. respectively. Single-line diagram representation for the Indian 118 bus EPDN is shown in Figure 5

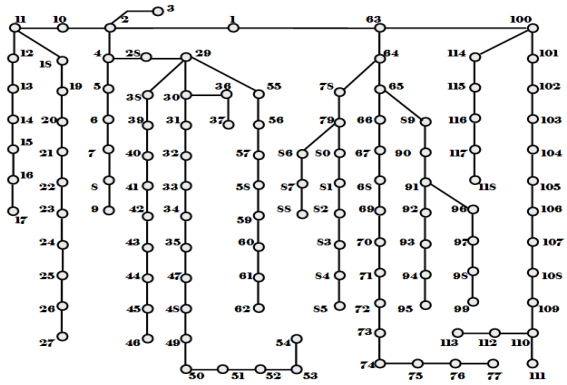

**Figure 5** Indian 118-bus test system – ICDN

**Table 7** Performance of SHOA considering load variations – Indian 118-bus

| Load level | **0.75 p.u.** | **1.0 p.u.** | **1.25 p.u.** |
|---|---|---|---|
| $P_{Loss\ (ACP)}$ / $P_{Loss\ (ICDN)}$ (kW) | 463.35 / 697.916 | 851.0121 / 1300 | 1377 / 2136.7134 |
| % $P_{Loss}$ reduction | 33.6095 | 34.3837 | 35.555 |
| $Q_{Loss\ (ACP)}$ / $Q_{Loss\ (ICDN)}$ (kVAr) | 348.725 / 527.4 | 632.644 / 979.045 | 1032.78 / 1604.615 |
| % $Q_{Loss}$ reduction | 33.87846 | 35.38152 | 35.6369 |
| Capacitor details (kVAr) | 925 (32)<br>450 (41)<br>1225 (50)<br>1050 (74)<br>750 (80)<br>750 (96)<br>150 (108)<br>1350 (111) | 1400 (32)<br>900 (41)<br>1850 (50)<br>1275 (74)<br>1025 (80)<br>700 (96)<br>225 (108)<br>1575 (111) | 1625 (32)<br>725 (41)<br>1850 (50)<br>1800 (74)<br>1200 (80)<br>1175 (96)<br>475 (108)<br>2100 (111) |
| % Cap. penetration | 52.06172 | 52.55102 | 51.4354 |
| $V_{min}$ (p.u) | 0.9315 | 0.9018 | 0.8788 |
| T × Δ $P_{Loss}$ Cost ($) | 25684.977 | 106522.403 | 69323.85 |
| T × Δ $Q_{Loss}$ Cost ($) | 6521.6375 | 27394.55 | 17393.315 |
| Cap. Inv. Cost ($) | | 60585 | |
| Net E G ($) | | **192255.7325** | |

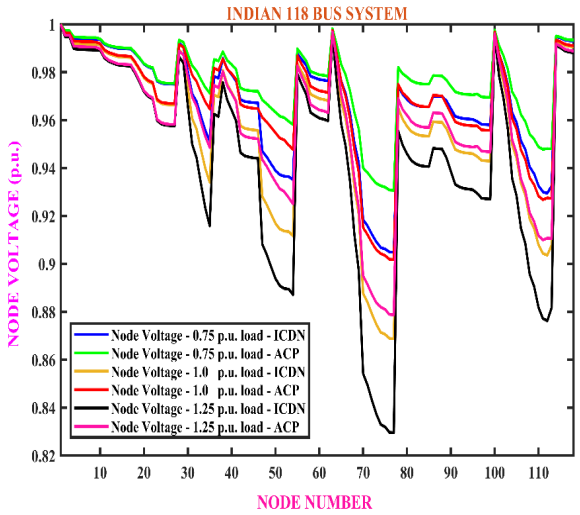


**Figure 6**. Bus Voltage profile enhancement – 3 load variations

The Indian 118 bus test system has been considered for the evaluation of RPS at eight optimal locations considering three different load variations (75%, 100%, and 125%). Table 7 depicts the performance of RPS under three load variations. The real and reactive power loss reductions are found to be between 33.6% and 35.6% respectively considering three load variations. The reactive power penetration varies between 51% and 52.5%. The bus voltage enhancement ACP considering LLV, MLV, and HLV are 0.02661, 0.033, and 0.049235 p.u. respectively. The net EG achieved by SHOA ACP is found to be $192255.7325 per year. Figure 6 depicts the performance of the bus voltage enhancements under ICDN and ACP considering three load variations.

Tables 8 to 10 reveal the performance comparison of SHOA with optimization techniques under LLV and MLV. From Table 8, it is witnessed that the performance of SHOA under LLV yields a better performance in terms of PLoss reduction and bus voltage enhancement compared to [8,9]. The reactive power penetration by the proposed method is found to be better than [8]. But QOSCA [9] yields less reactive power penetration compared to SHOA. The total number of locations for RPS considered by [8] is more than SHOA and a smaller number of locations for RPS by [9]. The bus voltage improvement is found to be better than [8].

**Table 8** Comparison of SHOA – Indian 118-bus DN – LLV (0.75 p.u.).

| Parameters | ISFS [8] | QOSCA [9] | SHOA |
|---|---|---|---|
| $P_{Loss\ (ACP)}$ / $P_{Loss\ (ICDN)}$ (kW) | 453.52 / 697.32 | 480.170/ 696.994 | 463.35 / 697.916 |
| % $P_{Loss}$ reduction | 34.96 | 31.10845 | 33.6095 |
| Capacitor details (kVAr) | 300 (24) 1150 (50)<br>600 (74) 300 (59)<br>950 (111) 700 (109)<br>400 (42) 400 (54)<br>550 (96) 750 (80)<br>600 (70) | 1500 (39)<br>350 (71)<br>950 (74)<br>1000 (91)<br>350 (106)<br>1400 (118) | 925 (32)<br>450 (41)<br>1225 (50)<br>1050 (74)<br>750 (80)<br>750 (96)<br>150 (108) 1350(111) |
| % Cap. penetration | 52.45316 | 43.45 | 52.06172 |
| T × $\Delta P_{Loss}$ Cost ($) | 26696.1 | 23742.228 | 25684.977 |
| Cap. Inv. Cost ($) | 40320 | 31470 | 38210 |
| Net E G ($) | -13623.9 | - 7727.772 | - 12525.023 |
| $V_{min}$ (p.u) | 0.9308 | 0.933 | 0.9315 |

**Table 9** Comparison of SHOA – Indian 118-bus DN – MLV (1.0 p.u.) – $P_{Loss}$ comparison.

| Parameters | SFS [8] | ISFS [8] | PODESCA [12] | SHOA |
|---|---|---|---|---|
| $P_{Loss}$ (ACP) / $P_{Loss}$ (ICDN) (kW) | 830.3155/1298.09 | 831.8988/1298.09 | 842.16 / 1297.95 | 851.0121 / 1300 |
| % $P_{Loss}$ reduction | 36.0356 | 35.91363 | 35.11615 | 34.3837 |
| Capacitor details (kVAr) | 1200 (34)<br>600 (42)<br>1500 (50)<br>500 (58)<br>1450 (74)<br>1250 (80)<br>900 (96)<br>1100 (107)<br>1350 (111) | 1000 (35)<br>600 (42)<br>1500 (50)<br>550 (58)<br>1450 (74)<br>1200 (80)<br>900 (96)<br>1000 (107)<br>1450 (111) | 50 (5)<br>1150 (34)<br>1500 (39)<br>600 (48)<br>1500 (74)<br>850 (86)<br>1200 (91)<br>1150 (109)<br>1150 (118) | 1400 (32)<br>900 (41)<br>1850 (50)<br>1275 (74)<br>1025 (80)<br>700 (96)<br>225 (108)<br>1575 (111) |
| % Cap. Penetration | 57.835 | 56.66116 | 53.72535 | 52.55102 |
| T × $\Delta P_{Loss}$ Cost ($) | 110979.5 | 110603.86 | 108136.1775 | 106522.403 |
| Cap. Inv. Cost ($) | 54830 | 53830 | 51330 | 49710 |
| Net E G ($) | **56149.5** | **56773.86** | **56806.1775** | **56812.403** |
| $V_{min}$ (p.u) | 0.9064 | 0.9063 | 0.9072 | 0.9018 |

**Table 10** Comparison of SHOA – Indian 118-bus DN – MLV – $P_{Loss}$ & $Q_{Loss}$ comparison.

| Parameters | SSO [10] | CSA [10] | ABC [10] | HMOO [10] | AEFA [11] | SCA [9] | QOSCA [9] | SHOA |
|---|---|---|---|---|---|---|---|---|
| $P_{Loss}$ (ACP) / $P_{Loss}$ (ICDN) (kW) | 830.15 / 1303.2 | 858.89 / 1303.2 | 854.39 / 1303.2 | 859.9 / 1303.2 | 859.86 / 1294.3 | 844.93 / 1297.413 | 841.259 / 1297.413 | 851.0121 / 1300 |
| % $P_{Loss}$ reduction | 36.3 | 34.09377 | 34.4391 | 34.01627 | 33.5656 | 34.8758 | 35.15874 | 34.53753 |
| $Q_{Loss}$ (ACP) / $Q_{Loss}$ (ICDN) (kVAr) | 621.51 / 1177.8 | 644.94 / 1177.8 | 639.08 / 1177.8 | 775.9 / 1177.8 | 651.73 / 976.54 | 631.42 / 978.715 | 630.331 / 978.715 | 632.644 / 979.045 |
| % $Q_{Loss}$ reduction | 47.2313 | 45.242 | 45.7395 | 34.123 | 33.2613 | 35.4848 | 35.596 | 35.38152 |
| Capacitor details (kVAr) | 1350 (6)<br>1350 (21)<br>1100 (32)<br>1300(39)<br>900 (40)<br>950 (47)<br>1300 (73)<br>1550 (82)<br>800 (90)<br>1100 (109)<br>1200 (110) | 1500 (32)<br>1500 (39)<br>550 (40)<br>950(70)<br>750 (74)<br>1050 (86)<br>1500 (108)<br>1200 (118) | 850 (32)<br>1050 (35)<br>1300 (40)<br>800 (50)<br>550 (70)<br>1300 (73)<br>1200 (79)<br>700 (105)<br>250 (106)<br>800 (109) 1200 (110) | 600 (20)<br>1650 (36)<br>650 (42)<br>550 (58)<br>850 (70)<br>850 (74)<br>1200 (80)<br>800 (97)<br>700 (104)<br>1800 (111) | 750 (22)<br>2050 (35)<br>700 (41)<br>1750 (50)<br>700 (58)<br>1000 (74)<br>2200 (80)<br>1700 (111) | 1500 (32)<br>1450 (39)<br>550 (43)<br>1400 (74)<br>700 (86)<br>1500 (91)<br>1500 (108)<br>1100 (118) | 1300 (32)<br>1500(39)<br>600 (43)<br>400 (71)<br>1100 (74)<br>950 (86)<br>1100 (91)<br>1250 (106)<br>1450 (118) | 1400 (32)<br>900 (41)<br>1850 (50)<br>1275 (74)<br>1025 (80)<br>700 (96)<br>225 (108)<br>1575(111) |
| %Cap. Penetration | 75.744 | 52.8446 | 58.71623 | 56.6616 | 63.7071 | 56.95474 | 56.66116 | 52.55102 |
| T × $\Delta P_{Loss}$ Cost ($) | 112231.113 | 105412.55 | 106480.17 | 105172.925 | 103070.89 | 107351.592 | 108222.537 | 106522.38 |
| T × $\Delta Q_{Loss}$ Cost ($) | 43993.2675 | 42140.345 | 42603.773 | 31783.592 | 25687.058 | 27465.2463 | 27551.368 | 27394.55 |
| Cap. Inv. Cost ($) | 71320 | 49960 | 56820 | 54450 | 59210 | 53460 | 53830 | 49710 |
| Net EG ($) | **84904.38** | **97592.895** | **92263.95** | **82506.517** | **69547.948** | **81356.8383** | **81943.905** | **84206.93** |
| $V_{min}$ (p.u) | 0.9145 | 0.906 | 0.9088 | 0.9292 | 0.901 | 0.906 | 0.906 | 0.9058 |

Tables 9 and 10 discuss the comparison between SHOA and [8, 12] in terms of PLoss with capacitor investment cost. However, Ref. [9 – 11] shows the comparison considering both PLoss and QLoss reduction with capacitor investment cost. From Table 9, it is apparent that the PLoss reduction obtained by SHOA is found to be less compared to [8,12]. The bus voltage enhancement ACP is found to be less compared to [8,12]. The reason for more PLoss reduction and better bus voltage enhancement is due to the increase in the number of RPS nodes and more reactive power penetration. However, the net EG yields by SHOA is better than [8,12].

Table 10 debates the performance of SHOA with [9 – 11]. The PLoss and QLoss reduction realized by SHOA is found to be less compared to [9, 10(SSO)]. The reason for excess PLoss and QLoss reduction is due to the increase in RPS nodes. From Table 10 it is obvious that the reactive power penetration by the proposed method is found to be less compared to [9 – 11] except HMOO and AEFA. Considering the total number of nodes for RPS and reactive power penetration, the bus voltage enhancement by SHOA is found to be better than [9 – 11]. Finally, the net EG optimized by SHOA is better than [9, 10(HMOO), 11]. However, due to more reactive power loss reduction, the net EG achieved by SSO, CSA, and ABC [10] are found to be better than SHOA.

## 5.0 CONCLUSIONS

This study utilizes the Sea Horse Optimization Algorithm (SHOA) to address the objective function combining real and reactive power loss reduction with capacitor investment expenses. This approach aims to maximize the EG across three distinct load variations. The benefits of employing SHOA are previously discussed and successfully applied for three radial DEPNs such as 28-bus PEA, Thailand, Indian 118 bus, and PG&E 69-bus DNs. Key observations include:

1. In general, previously published papers consider minimizing $P_{Loss}$ reduction with capacitor purchase and its associated cost. Apart from real power loss reduction, this paper considers $Q_{Loss}$ reduction as one of the objectives.

2. This paper has not employed any Sensitivity Factor-based indices for optimal buses requiring RPS. Instead, SHOA has to optimize both appropriate buses and the optimal sizing for RPS.

3. Significant reductions in overall power loss (% $P_{Loss}$) ranging from 33% to 37% have been observed across the three load variations for PG&E 69-bus DN. For the 28-bus PEA, Thailand DN, $P_{Loss}$ reduction is about 29% to 30% respectively for the two load variations. Similarly, around 33% to 35% of real power loss reduction has been witnessed in the case of the Indian 118-bus DN considering three load variations.

4. Considering the PG&E 69-bus and Indian 118-bus DEPN, the performances have been compared with the recent techniques presented in the literature. The difference in $P_{Loss}$ and $Q_{Loss}$ reduction achieved by SHOA is found to be better and even more significant. Upon evaluating the SHOA's performance on the aforementioned test systems, it is evident that SHOA outperforms other optimization algorithms in terms of achieving more EGs. However, SHOA's effectiveness in enhancing the bus voltage profiles has been comparatively lower.

## Nomenclature

| | |
|---|---|
| $P^{LT}$, $Q^{LT}$ | Total real and reactive power loss |
| ICDN | Initial Condition of the DN |
| $T_l$ | Time duration at $l^{th}$ load level (Hrs.) |
| $N_{LV}$ | Number of Load Variations |
| ACP | After Capacitor Placement |
| NQN | Number of compensation buses |
| ES | Energy Source (main) |
| TD | Total reactive power Demand (kVAr) |
| $Q_C$ | Capacitor size (kVAr) |
| $C_{Cap}$ | Capacitor Purchase Cost ($) |
| $C_{ins}$, $C_{O\&M}$ | Cap. installation, Operation & maintenance cost ($) |
| $N_{QN}$ | Number of reactive power compensation nodes |
| LLV, MLV, HLV | Light, Medium & Heavy Load Variations |
| $C_{QL}$ | Cost of the reactive energy from ES ($) |
| $V_i$ | The voltage at the $i^{th}$ node (p.u.) |

## Acknowledgement

Our sincere gratitude to Mr. K. Karthikeyan, Senior Engineer, Tagore Medical College & Hospital, Rathinamangalam, CHENNAI, INDIA for his endless support during my research work, without whom I would not have been in this present position.

## Conflicts of Interest

The authors declare that they have no known competing financial interests or personal relationships that could have appeared to influence the work reported in this paper.

## References

[1] Abdelaziz, A., Mohamed, F., Mekhamer, S., & Badr, M. 2010. Distribution system reconfiguration using a modified Tabu Search algorithm. *Electrical Power System Research.* 80: 943–953.

[2] Abdelaziz, A., Ali, E., & Elazim, S. A. 2016. Optimal sizing and locations of capacitors in radial distribution systems via flower pollination optimization algorithm and power loss index. *Engineering Science and Technology an International Journal,* 19: 610–618.

[3] Teimourzadeh, H., Mohammadi-Ivatloo, B., & Farzamnia, A. 2019. Wild Goats Optimization Approach for Capacitor Placement Problem. *The International Journal of Integrated Engineering.* 11(4): 31–39.

[4] Montoya, O. D., Gil-González, W., & Garcés, A. 2022. On the Conic Convex Approximation to Locate and Size Fixed-Step Capacitor Banks in Distribution Networks. *Computation*, 10: 32.

[5] Gil-González, W., Montoya, O. D., Rajagopalan, A., Grisales-Noreña, L. F., & Hernández, J. C. 2020. Optimal Selection and Location of Fixed-Step Capacitor Banks in Distribution Networks Using a Discrete Version of the Vortex Search Algorithm. *Energies.* 13: 4914.

[6] Riaño, F. E., Cruz, J. F., Montoya, O. D., Chamorro, H. R., & Alvarado-Barrios, L. 2021. Reduction of Losses and Operating Costs in Distribution Networks Using a Genetic Algorithm and Mathematical Optimization. *Electronics,* 10: 419.

[7] Kien, L. C., Nguyen, T. T., Pham, T. D., & Nguyen, T. T. 2021. Cost reduction for energy loss and capacitor investment in radial distribution networks applying novel algorithms. *Neural Computing and Applications*. 33(22): 15495 -15522. DOI: 10.1007/s00521-021-06172-7.

[8] Nguyen, P. T., Anh, T. N., Ngoc, D. V., & Thanh, T. L. 2020. A Cost-Benefit Analysis of Capacitor Allocation Problem in Radial Distribution Networks Using an Improved Stochastic Fractal Search Algorithm. *Complexity,* 2020: 1-32., Article ID 8811674.

[9] Biswal, S. R., & Shankar, G. 2021. A Novel Quasi-opposition Based Sine Cosine Algorithm for Optimal Allocation and Sizing of Capacitor in Radial Distribution Systems. *Research Square.* DOI: https://doi.org/10.21203/rs.3.rs-1070297/v1

[10] Danish, S. M. S., Ahmadi, M., Yona, A., Senjyu, T., Krishna, N., & Takahashi, H. 2020. Multi-objective optimization of optimal capacitor allocation in radial distribution systems. *International Journal of Emerging Electrical Power Systems,* 21(3): 1-11. article 20190206.

[11] Abdelsalam, A. A. A., & Gabbar, H. A. 2019. Shunt Capacitors Optimal Placement in Distribution Networks Using Artificial Electric Field Algorithm. *7th International Conference on Smart Energy Grid Engineering.*

[12] Mahfoud, R. J., Alkayem, N. F., Sun, Y., HaesAlhelou, H., Siano, P., & Parente, M. 2020. Improved Hybridization of Evolutionary Algorithms with a Sensitivity-Based Decision-Making Technique for the Optimal Planning of Shunt Capacitors in Radial Distribution Systems. *Applied Sciences,* 10: 1384.

[13] Muhtazaruddin, M. N., Jamian, J. J., Nguyen, D., Jalalludin, N. A., & Fujita, G. 2014. Optimal capacitor placement and sizing via artificial bee colony. *International Journal of Smart Grid and Clean Energy,* 3(2): 200-206.

[14] Haldar, V., & Chakraborty, N. 2015. Power loss minimization by optimal capacitor placement in radial distribution system using modified cultural algorithm. *International Transactions on Electrical Energy — Systems,* 25(1): 54-71.

[15] Srinivasan, G., Amaresh, K., & Cheepati, K. R. 2022. Economic based evaluation of DGs in capacitor allocated optimal distribution network. *Bulletin of the Polish Academy of Sciences: Technical Sciences,* 70(1): 1-10.

[16] S. Sultana & P. K. Roy, 2014."Multi-objective quasi-oppositional teaching learning based optimization for optimal location of distributed generator in radial distribution systems," *Electrical Power and Energy System,* 63: 534–545.

[17] R. K. Viral & D. K. Khatod, 2012. "Optimal planning of Distributed Generation systems in distribution system: A review," *Renewable and Sustainable Energy Reviews,* 16: 5146–5165.

[18] S. M. Abd-Elazim & E. S. Ali, "A hybrid Particle Swarm Optimization and Bacterial Foraging for optimal Power System Stabilizers design," *Electrical Power and Energy Systems*, 46: 334–341, 2013.

[19] D. Prakash & C. Lakshminarayana, 2017. "Optimal siting of capacitors in radial distribution network using whale optimization algorithm," *Alexandria Engineering Journal,* 56(4): 499–509.

[20] Ola Badran, Hazlie Mokhlis, Saad Mekhilef and Wardiah Dahalan, 2018. Multi-Objective Network Reconfiguration with Optimal DG Output Using Meta-Heuristic Search Algorithms, *Arabian Journal of Science and Engineering,* 43: 2673–2686, DOI: 10.1007/s13369-017-2714-9

[21] Jafar Jallad, Saad Mekhilef, Hazlie Mokhlis , Javed Laghari and Ola Badran, 2018. Application of Hybrid Meta-Heuristic Techniques for Optimal Load Shedding Planning and Operation in an Islanded Distribution Network Integrated with Distributed Generation, *Energies.* 11: 1134. DOI:10.3390/en11051134.

[22] Farah Ramadhani, Mohammad Azlan Hussain, Hazlie Mokhlis, and Hazlee Azil Illias, 2021. Two-stage fuzzy-logic-based for optimal energy management strategy for SOFC/PV/TEG hybrid polygeneration system with electric charging and hydrogen fueling stations, *Journal of Renewable Sustainable Energy, 1*3: 024301. DOI: https://doi.org/10.1063/5.0010832

[23] S. Zhao, T. Zhang, S. Ma, & M. Wang, 2023. "Sea-horse optimizer: a novel nature-inspired meta-heuristic for global optimization problems," *Applied Intelligence*. 53: 11833–11860,

[24] T. Ramana, V. Ganesh, & S. Siranagaraju, 2003. "Simple and Fast Load Flow Solution for Electrical Power Systems," *International Journal of Electrical Engineering and Informatics*, 5(5): 245-253.

[25] V. Kumar, S. Swapnil, R. Ranjan, & V. R. Singu, 2017. "Improved Algorithm for Load Flow Analysis of Radial Distribution System," *Indian Journal of Science and Technology*, 10(18): 1-7.

[26] B. Venkatesh & R. Ranjan, 2003. "Data structure for radial distribution load flow analysis," *IEEE Proceedings on Generation. Transmission and Distribution.* 150(1): 101-106.

[27] H. Karimi & R. Dashti, 2016. "Comprehensive framework for capacitor placement in distribution networks from the perspective of distribution system management in a restructured environment," *Electrical Power and Energy Systems,* 82: 1–18,

[28] I. Pérez Abril, 2017. "Algorithm of inclusion and interchange of variables for capacitors placement," *Electric Power System Research* 148: 117-126, [Online]. DOI: https://doi.org/10.1002/2050-7038.12377

[29] N. Rugthaicharoencheep & S. Sirisumrannukul, 2008."Benefit Assessment of Loss Reduction from Distributed Generation in Distribution Networks by Tabu Search," C*onference of The electric Power Supply Industry (CEPSI),* 669].